Water Management in the Cathode Side of a PEM Fuel Cell

N. Khajeh-Hosseini D.[i], H. R. Shabgard [ii] and M. J. Kermani[iii] *

ABSTRACT

A one dimensional isothermal mathematical modeling of cathode side of a Proton Exchange Membrane (PEM) fuel cell is developed for the water management problem. Water transport is investigated in both cathode Gas Diffusion Layer (GDL) and membrane through solving appropriate equations for fluid flow and mass transport in GDL and water transport within the membrane. The gaseous mixture flowing in cathode GDL consists of three species: oxygen, water vapor and nitrogen. The model considers one phase flow in the gas diffusion layer and then predicts the regions with possible condensation. Homogenous distribution of wet phase (liquid water) is assumed throughout each wet control volume as fog. The model couples all governing equations in both membrane and GDL using an innovative algorithm. A detailed discussion of numerical techniques for the PEMFC model is given with a flow diagram to provide an overview of the solution procedure. Validation for polarization curve is implemented to show agreement between the obtained results and existing results in the literature.

KEYWORDS

PEM fuel cell, Water management, Porous electrode, Stefan-Maxwell equation.

1. INTRODUCTION

A one dimensional and isothermal mathematical model of cathode side of a PEMFC is presented for handling water management problem. Water management is one of the critical issues in the performance modeling of a PEMFC. At high cell current densities, excessive water transport throughout the membrane and water production in the cathode catalyst layer result in mass transport limitations and flooded GDL gas pores with water. At low cell current densities membrane dehydration may occurs at the anode side resulting in membrane ohmic losses. These losses cause reduction of the PEMFC performance. Membrane is considered to be partially hydrated.

Bernardi and Verbrugge [1] presented a 1D and isothermal model and evaluated the necessitated water for adding or omitting from the cathode side to keep the membrane fully hydrated. They assumed the water phases (liquid + vapor) equilibrium in GDL. Fuller and Newman [2] developed a pseudo 2D model that considers both water and thermal management. Springer et al. [3] developed a 1D and isothermal model under two different water transport mechanisms; electro-osmotic drag and back-diffusion. They also assumed water phase's equilibrium. You and Liu [4] developed a two phase model for the gas mixture in the GDL. In this paper, a one phase model is proposed to predict the regions with possible condensation.

The key idea that is used for handling water management is introducing a parameter named the net water transport coefficient throughout the membrane, α. α couples all of the governing equations at the catalyst layer and GDL interface. A detailed discussion of the numerical techniques for the cathode side water management is given with the flow diagram to provide an overview of the solution procedure.

2. PROBLEM DESCRIPTION

The computational domain is depicted in Fig. 1. The model consists of gas channel, gas diffusion layer, cathode catalyst layer and membrane. The interfaces between the GDL and membrane are impregnated with a platinum catalyst and are called catalyst layer (CL). Oxygen and water molar fluxes direction are also shown in Fig. 1.

---

i Graduate Student of Energy Conversion, Amirkabir University of Technology.   E-mail: navvabk@yahoo.com
ii Lecture, Islamic Azad University, Mashhad branch.   E-mail: hamid20369@yahoo.com
iii * Corresponding Author, Assistant Professor of Thermo-Fluid, Also Head of Energy Research Lab. E-mail: mkermani@aut.ac.ir

3. GOVERNING EQUATIONS

A. Governing Equations in GDL

Governing equations for transient condition of a mixture consisting of 1: Oxygen, 2: Steam (liquid +vapor), 3: Nitrogen, are as follow. Density (kg/m^3) and concentration (mol/m^3) are evaluated at the total volume (wet + dry). In fact homogenous distribution of wet phase (liquid water) will be assumed throughout each wet control volume as fog.
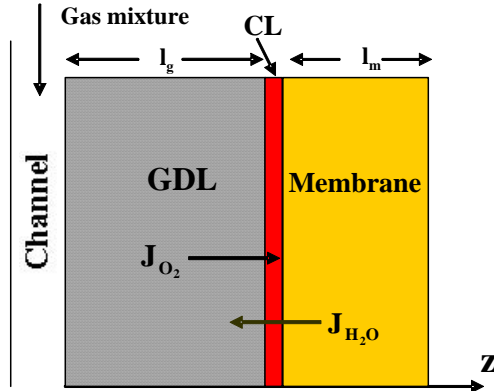

Figure 1: Schematic of the computation domain.

Porous electrode (GDL) equations consist of the continuity equation as well as conservation equations for species and Darcy's law as the momentum equation.

At any location in the GDL the total mass of the gas mixture is conserved by

$$\frac{\partial \rho}{\partial t} + \nabla.(\rho \upsilon) = 0 \tag{1}$$

where ρ and υ are the gas mixture density and velocity.

The species conservation equation for the oxygen and steam are given as:

$$\frac{\partial C_1}{\partial t} + \nabla.(C_1 \upsilon + J_1) = 0 \tag{2}$$

$$\frac{\partial C_2}{\partial t} + \nabla.(C_2 \upsilon + J_2) = 0 \tag{3}$$

where C_1 and C_2 denote species molar concentrations for components 1 and 2 at the total volume of the void spaces as a result of homogenous assumption. J_1 and J_2 are the molar diffusive fluxes. In serpentine flow field design, diffusion is the dominant phenomena in mass transport through the GDL.

Darcy's law is used for describing the gas mixture flow in the GDL:

$$\upsilon = -\frac{K}{\varepsilon \mu} \nabla P \tag{4}$$

where K, μ and P denote the permeability, gas mixture viscosity and pressure respectively. ε is the GDL porosity and is used to relate the pore gas velocity, υ, to the average velocity, $\varepsilon \upsilon$. Diffusive fluxes J_1 and J_2 are modeled with the Stefan-Maxwell equation for ternary gas mixture [5]

$$\begin{bmatrix} J_1 \\ J_2 \end{bmatrix} = -\begin{bmatrix} a & b \\ c & d \end{bmatrix} \begin{bmatrix} \nabla \left(C_1 / C \right) \\ \nabla \left(C_2 / C \right) \end{bmatrix} \tag{5}$$

in which the coefficient matrix is given as:

$$\begin{aligned}
a &= C\left[s_{11} D_{11}^{eff} + s_{12} D_{21}^{eff} \right] \\
b &= C\left[s_{11} D_{12}^{eff} + s_{12} D_{22}^{eff} \right] \\
c &= C\left[s_{21} D_{11}^{eff} + s_{22} D_{21}^{eff} \right] \\
d &= C\left[s_{21} D_{12}^{eff} + s_{22} D_{22}^{eff} \right]
\end{aligned} \tag{6}$$

where D_{ij}^{eff} is the effective binary diffusivity of species i in j and is related to its bulk value through the Bruggeman correlation [6]

$$D_{ij}^{eff} = \varepsilon^{1.5} D_{ij} \tag{7}$$

with the binary diffusivity $D_{ij}(T_0, P_0)$ evaluated at the given pressure P_0 and temperature T_0, $D_{ij}(T, P)$ will be obtained by [7]

$$D_{ij}(T,P) = D_{ij}(T_0, P_0)\left(\frac{P_0}{P}\right)\left(\frac{T}{T_0}\right)^{1.75} \tag{8}$$

In (6), s_{ij} is given as following:

$$s_{ij} = \delta_{ij} - \frac{C_i}{\rho}\left(M_j - M_3\right) \qquad i,j = 1,2 \tag{9}$$

where Kronecker delta, δ_{ij}, is equal to 1 when $i = j$ and is zero otherwise. To close the system of equations in the GDL, it is assumed that the gas mixture obeys the ideal gas law

$$P = C\overline{R}T \tag{10}$$

where $\overline{R}$ and T are respectively the universal gas constant and temperature. The nitrogen molar concentration in the cathode GDL is obtained by

$$C_3 = C - C_1 - C_2 \tag{11}$$

Gas mixture density is related to species concentration via

$$\rho = C_1 M_1 + C_2 M_2 + C_3 M_3 \tag{12}$$

where M denotes the molecular weight.

Liquid saturation, s_l, in the GDL shows the fraction of total pores occupied by liquid water in the porous electrode. In the present model, liquid water is generated as soon as the saturation line is crossed [8]

$$s_l = \frac{P_w - P_w^{sat}}{\frac{\overline{R}T}{M_w}\rho_w^L - P_w^{sat}} \tag{13}$$

where P_w is the partial pressure of water vapor and P_w^{sat} is the saturation pressure obtained at the mixture temperature T:

$$\begin{aligned}
\log_{10} P_W^{sat} &= -2.1794 + 0.02953(T - 273.15) - 9.1837 \times \\
&10^{-5} \times (T - 273.15)^2 + 1.4454 \times 10^{-7} \times (T - 273.15)^3
\end{aligned} \tag{14}$$

In the above equation, P_w^{sat} and T are in terms of atmosphere and Kelvin, respectively.

B. Governing Equations in Membrane

Water transports through the membrane via three mechanisms: 1) electro-osmotic drag, 2) back diffusion and 3) hydraulic permeability, as shown in Fig. 2.
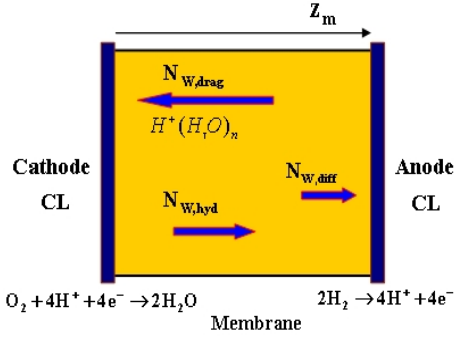

Figure 2: Schematic of the different water transport mechanisms through the membrane.

The net flux of water across the membrane is obtained by:

$$N_{w,net} = N_{w,drag} - N_{w,diff} - N_{w,hyd} \qquad (15)$$

Electro-osmotic drag induced by protons migration from anode side to the cathode side (the negative direction) and is expressed [3]

$$N_{w,drag} = \frac{2.5}{22} \lambda \frac{I_\delta}{F} \qquad (16)$$

where I_δ and F are the cell current density and Faraday's constant. λ denotes the membrane water content and is given by Springer et al. [3] at different ranges of water activity a,

$$\begin{aligned}
\lambda &= 0.043 + 17.81a - 39.85\,a^2 + 36a^3 && (0 < a \le 1) \\
\lambda &= 14 + 1.4(a-1) && (1 < a \le 3) \\
\lambda &= 16.8 && (a > 3)
\end{aligned} \qquad (17)$$

where water activity, a, is defined in terms of water mole fraction x_w, mixture pressure P and water saturation pressure P_w^{sat} as:

$$a = x_w \frac{P}{P_w^{sat}} \qquad (18)$$

Back diffusion is induced by water concentration difference in the opposite direction of electro-osmotic drag (see Fig. 2) and is given by [9]

$$N_{w,diff} = \frac{\rho_M}{M_M} D_{W,F} \frac{d\lambda}{dz} \qquad (19)$$

where ρ_M and M_M are the dry membrane (Nafion-117) density and membrane equivalent weight, respectively. $D_{W,F}\ (cm^2/s)$ is the Fickian diffusion coefficient of water within the membrane and is a function of water content and temperature:
for ($0 < \lambda \le 3$)

$$D_{W,F} = 3.1 \times 10^{-3} \lambda \left(-1 + \exp(0.28\lambda)\right) \times \exp\left(-\frac{2436}{T}\right) \qquad (20)$$

and for ($3 < \lambda < 17$)

$$D_{W,F} = 4.17 \times 10^{-4} \lambda \left(1 + 161\exp(-\lambda)\right) \times \exp\left(-\frac{2436}{T}\right) \qquad (21)$$

Hydraulic permeation is induced by gas pressure difference between the anode side and cathode side of the membrane and its corresponding flux is assumed in the positive direction, as shown in Fig. 2. Water flux due to hydraulic permeation is given by [4]

$$N_{w,hyd} = \frac{\rho_M}{M_M} \lambda \frac{K_M}{\mu_W} \frac{dP}{dz} \qquad (22)$$

where K_M and μ_W are the membrane hydraulic permeability and water dynamic viscosity respectively.

It is important to note that ρ_M/M_M in (19) and $\rho_M \lambda/M_M$ in 22 are corresponding to fixed charged site (SO_3^-) concentration and water concentration within the membrane, as well.

Substituting (16), (19) and (22) into (15) gives:

$$N_{w,net} = \frac{2.5}{22} \lambda \frac{I_\delta}{F} - \frac{\rho_M}{M_M} D_{W,F} \frac{d\lambda}{dz} - \frac{\rho_M}{M_M} \lambda \frac{K_M}{\mu_M} \frac{dP}{dz} \qquad (23)$$

According to Fig. 2 positive $N_{w,net}$ shows the net water transport from anode side to the cathode side.

C. Governing Equations in cathode catalyst layer

The transport of species within the CL is considered solely due to the concentration gradient, which is described by the Fick's law of diffusion

$$\frac{dC_{O_2}}{dz} = \frac{i - I_\delta}{4\,F\,D_{O_2}^{eff\cdot}} \qquad (24)$$

in which C_{O_2}, i and $D_{O_2}^{eff}$ are respectively oxygen concentration, protonic current density and oxygen diffusion coefficient. Here, in the catalyst layer the electrochemical reaction occurs according to

$$O_2 + 4H^+ + 4e^- \rightarrow 2H_2O \qquad (25)$$
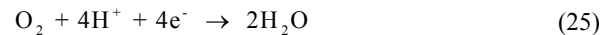
The electrochemical reaction rate is obtained using the Butler-Volmer equation

$$\frac{di}{dz} = a.i_0 \left[\exp\left(\frac{\alpha_c F}{RT} \eta_{act}\right) - \exp\left(-\frac{\alpha_a F}{RT} \eta_{act}\right) \right] \qquad (26)$$

where i_0 is the exchange current density, experimentally determined for smooth-surface reaction sites, and a is the specific area of the reaction sites. α_c and α_a are cathodic and anodic charge transfer coefficient considered as one [1]. Potential drop within the catalyst layer occurs due to following reasons: (1) electron transport through the solid portion of the catalyst layer, (2) proton transport through the membrane phases of the catalyst layer. The activation overpotential within the CL are caused by these drops according to

$$\frac{d\eta_{act}}{dz} = \frac{i}{\kappa^{eff}} + \frac{i - I_\delta}{\sigma^{eff}} \tag{27}$$

where κ^{eff} and σ^{eff} are the effective electrical and protonic conductivity corresponding to the solid and membrane phase of catalyst layer.

4. BOUNDARY CONDITIONS

The boundary conditions used in the present study are described based on the schematic picture of Fig. 1. The geometry consists of three regions: GDL, CL and membrane and four boundaries as: the interfaces of channel/ GDL, GDL/catalyst layer, catalyst layer/membrane and the right end of the membrane as shown in Fig. 1. It is important to note that the interface between catalyst layer and membrane is for solving the set of differential equations of (24), (26) and (27), and generally it has no role on water management. These boundary conditions are described below.

A. Gas Channel/GDL interface (i.e. at z = 0)

The inlet velocity υ_{in} is a function of the cell current density I_δ and oxygen stoichiometric flow ratio ζ, MEA area, A_{MEA}, and channel cross-section area, A_{ch}, that is

$$\upsilon_{in} = \xi \frac{I_\delta}{4F} \frac{A_{MEA}}{A_{ch}} \frac{1}{x_{O_2,in}} \frac{\overline{R}T}{P_c} \tag{28}$$

where $x_{O_2,in}$ and P_c are the oxygen mole fraction and cathode gas mixture pressure at the channel inlet. Stoichiometric flow ratio, ξ, is defined as the amount of reactant in the chamber gas feed divided by the amount required by the electrochemical reaction. Oxygen is consumed at the cathode catalyst layer reaction and its consumption flux is (see Fig. 1) [10]:

$$N_{O_2} = \frac{I_\delta}{4F} \tag{29}$$

The molar flux of the water transported through the GDL and toward the channel is the sum of water generated within the cathode catalyst layer and net water transported through the membrane (shown in Fig. 1):

$$N_{H_2O} = -\left(N_{w,net} + \frac{I_\delta}{2F} \right) \tag{30}$$

With the known oxygen and water flux at the GDL/Catalyst layer interface as shown in Fig. 1, using material balance along the gas channel, average values for the oxygen and water concentration along the gas channel would be obtained. These values are used as the boundary conditions at the gas channel/GDL interface. Those are,

$$\overline{C}_{O_2} = C_{O_2,in} - \frac{1}{2\upsilon_{in}} \frac{I_\delta}{4F} \frac{A_{MEA}}{A_{ch}} \tag{31}$$

$$\overline{C}_W = C_{W,in} - \frac{1}{2\upsilon_{in}} \left(N_{w,net} + \frac{I_\delta}{2F} \right) \frac{A_{MEA}}{A_{ch}} \tag{32}$$

where $C_{O_2,in}$ and $C_{W,in}$ are the oxygen and water vapor concentration at the channel inlet and are given by:

$$C_{O_2,in} = x_{O_2,in} \frac{P}{\overline{R}T} \tag{33}$$

$$C_{W,in} = \phi_{in} \frac{P_W^{sat}}{\overline{R}T} \tag{334}$$

where ϕ_{in} is the relative humidity of the cathode gas mixture at the entrance of the channel.

B. GDL/CL interface (i.e. at z = l_g)

The oxygen and water molar flux at this interface can be expressed by (25) and (26). The mixture velocity at the GDL/CL interface is

$$\upsilon = \frac{M_{O_2} N_{O_2} + M_{H_2O} N_{H_2O}}{\varepsilon \rho} \tag{35}$$

where M_{O_2} and M_{H_2O} are the oxygen and water molecular weight. Considering species fluxes through this interface (represented by (25) and (26)) and applying flux 1: oxygen and 2: water respectively in (2) and (3), gives

$$N_{O_2} = C_1 \upsilon + J_1 \tag{36}$$

$$N_{H_2O} = C_2 \upsilon + J_2 \tag{37}$$

The oxygen concentration in the GDL/CL interface is calculated using the Henry's Law [1]

$$C_{O_2} = \frac{P_{O_2}}{H_{O_2}} \tag{38}$$

where P_{O2} is the partial pressure of oxygen gas calculated from GDL equations. At this boundary since the protinic current density is zero, then,

$$i = 0 \tag{39}$$

C. CL/Membrane interface (i.e. at z = l_g + l_c)

l_c is the catalyst layer thickness. The protonic current density i at this boundary approaches to its ultimate value, i.e. the cell current density I_δ.

D. The right boundary of the membrane (i.e. at z = l_g+l_c+l_m)

At the right boundary of the membrane, total pressure is taken to be equal to anode side pressure with the relative humidity of 100%. Therefore, the water activity, a, is set equal to 1 at this interface.

5. SOLUTION PROCEDURE

In order to implement the water management, it is noted that the model equations developed above for the GDL and membrane are coupled with the boundary conditions at the GDL/CL interface. The key idea for handling the solution procedure is introducing the dimensionless parameter that shows the net water transported through the membrane that couples the governing equations

$$\alpha = N_{w,net} \frac{F}{I_\delta} \tag{40}$$

α is guessed at the GDL/CL interface. Then governing

equations are solved over the GDL and membrane. The net water transported through the membrane gives the new α. The solution is considered to be convergent when the error for α between two successive iterations becomes small enough.

The flow-chart shown in Fig. 3 presents a step by step approach to obtain the results. The numerical data needed to solve the differential equations for water management i.e. in the GDL and Membrane are summarized in Table 1 while the parameters needed to solve ordinary differential equations of CL are listed in table 2.

6. RESULTS

In Fig. 4, a comparison of the present computational result and the experimental result of Ticianelli et al. (1988) [12] has been shown. This Figure shows cell potential versus output cell current density. Cell potential is obtained from subtracting overpotentials in CL and membrane from reversible voltage [1],

$$V_c = E_{rev} - \eta_{act} - R I_\delta \qquad (41)$$

E_{rev} and R in this calculation are 1.01 volt and 0.23 Ωcm^2. As shown in this figure, the good agreement between the present computation and the experimental data is obtained.

Fig. 5 shows the distribution of the oxygen mole fraction within the GDL at three different values of cell current densities. Mole fraction is defined as the ratio of the species concentration to the total concentration. At high cell current densities, oxygen consumption rate increases (see (25)), thus its corresponding molar flux decreases more comparing with low cell current densities. Combining (31) and (33) shows that average oxygen concentration is a function of the gas mixture pressure, P, oxygen inlet mole fraction, $x_{O_2,in}$, and oxygen stoichiometric flow ratio, ζ, at the cathode channel inlet. Since these values are constant at all cell current densities, average oxygen concentration and oxygen mole fraction are constant at $z_g = 0$.

TABLE 1
DATA TAKEN FROM THE LITERATURE FOR THE VALUES USED IN THE COMPUTATION OF GDL AND MEMBRANE.

Fuel cell temprature, T, (*Kelvin*)	353
Cathode side pressure, P_c (*atm*)	5
Anode side pressure, P_a (*atm*)	3
GDL thickness, l_g, (*m*)	2.6×10^{-4}
Membrane thickness, l_m, (*m*)	2.3×10^{-4}
Area ratio, A_{MEA}/A_{ch}	312
GDL permeability, K, (*m²*)	1.76×10^{-11}
Membrane permeability, K_M, (*m²*)	1.8×10^{-18}
Porosity, ε	0.4
Dynamic viscosity of water, μ_W, (*Pa.s*)	3.565×10^{-4}
Dry membrane density, ρ_M, (*Kg/m³*) [11]	2.16×10^3
Ionomer equivalent weight, M_M, (*Kg/m³*)	1100

TABLE 2
DATA TAKEN FROM THE LITERATURE FOR THE VALUES USED IN THE COMPUTATION OF CL

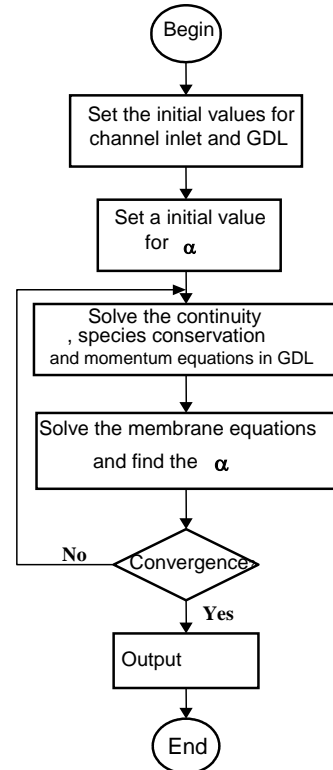|	
CL thickness, l_c, (*m*)	50×10^{-6}
Protonic conductivity, κ^{eff} *(1/Ω-m)*	17
Electronic conductivity, σ^{eff} *(1/Ω-m)*	7.27×10^4
Oxygen diffusion coefficient, D_{O2}^{eff} *(m²/s)*	9.19×10^{-9}
Reaction surface area times exchange current density, ai_0 *(A/m³)*	500

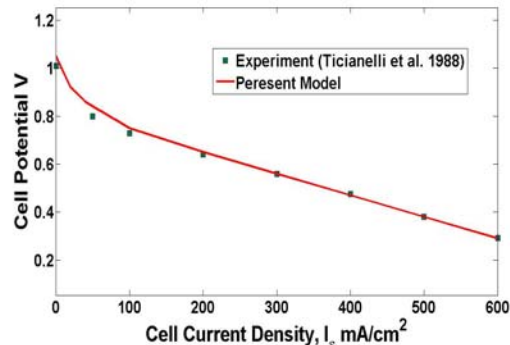Figure 3: Flow-chart of solution.

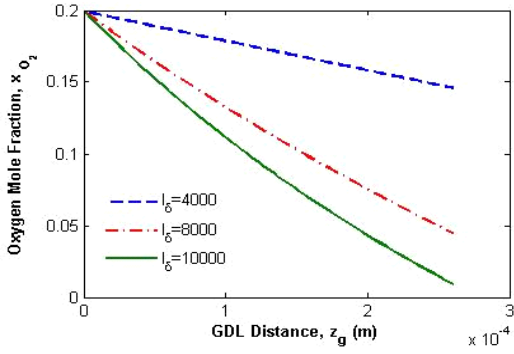Figure 4: Comparison between Polarization Curve of Experiment, Ticianelli et al. [12] and present study.

Figure 5: Distribution of the oxygen mole fraction through the cathode gas diffusion layer, $(0 < z_g < l_g)$ at different cell current densities, I_δ (A/m^2).

Fig. 6 shows the distribution of the water mole fraction within the GDL at three different values of cell current densities. It can be seen that at low cell current density, water mole fraction decreases and at high cell current density, it increases. This figure i.e. Fig. 6 can be explained noticing the direction of water flux N_{H_2O}. At low cell current density, α shows that water is transported from the cathode side of the membrane (membrane/CL interface) toward the anode side (The right boundary of the membrane. Thus, water goes outside of the cathode side and its mole fraction will be decreased. On the other hand, following result indicates that water will be transported from the anode side of the membrane (The right boundary of the membrane) toward the cathode side (membrane/CL interface). Thus, input water to the GDL results in increasing water mole fraction and accumulation of water in the GDL.
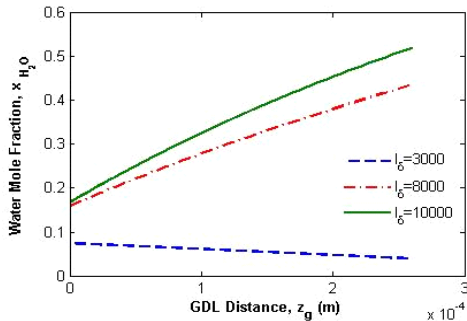

Figure 6: Distribution of the water mole fraction through the cathode gas diffusion layer, $(0 < z_g < l_g)$ at different cell current densities, I_δ (A/m^2).

Fig. 7 depicts the profile of the average gas mixture velocity, $\varepsilon\upsilon$, within the GDL at two values of cell current densities near the threshold value. Fig. 7 indicates that approximately at $I_\delta = 3825$ A/m^2 the bulk motion direction of the mixture at the GDL is reversed. Positive $\varepsilon\upsilon$ at high I_δ demonstrates the bulk motion of the gas mixture toward the channel.
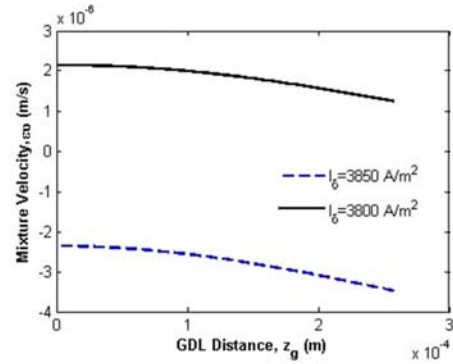

Figure 7: Average gas mixture velocity through the GDL $(0 < z_g < l_g)$ at two different cell current densities.

Fig. 8 displays the variation of net water molar flux across the membrane and its corresponding components at the cell current density of $I_\delta = 8000$ A/m^2. Water flux due to electro-osmotic drag variation is proportional to the water content variation within the membrane. Water content increases with water activity a (see 17). Since in this study, only the cathode side is considered, water activity at the right boundary of the membrane (i.e. at $z = l_g + l_c + l_m$) is set $a = 1$. This means that water is considered at its saturated condition (see 18) at $z = l_g + l_c + l_m$. The electro-osmotic flux $N_{W,drag}$ decreases slightly along the membrane because of the decrease of water content in the membrane. Fig. 8 also shows the higher activity at the cathode side of the membrane rather than the anode side. The water that is produced at the cathode catalyst layer and is transferred from the membrane causes the high water concentration at the cathode side of the membrane. There is a diffusion water flux $N_{W,diff}$ from the cathode side to the anode side as a result of water concentration difference.
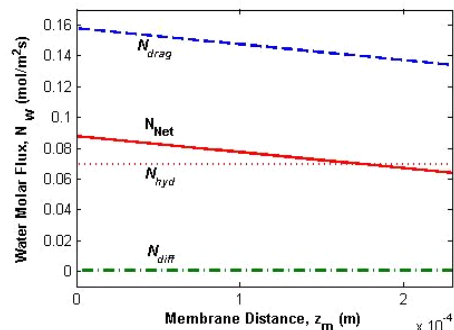

Figure 8: The electro-osmotic, net, diffusion and hydraulic permeation water fluxes across the membrane at $I_\delta = 8000$ (A/m^2) ,$(0 < z_m < l_m)$.

Combining the above three water transport mechanisms, the net water transport coefficient is depicted as a solid line in Fig. 8. The net water transport flux decreases along the membrane, due to the electro-

osmotic drag flux reduction. It can be also found that $N_{W,drag}$ has the main contribution to $N_{w,net}$.

Fig. 9 shows the liquid water saturation variation through the GDL at different cell current densities. In the present model liquid water is generated once the saturation line is crossed. In the other word, when the partial pressure of the water vapor P_w is greater than the saturated vapor pressure. In this case, the rate of condensation is proportional to the difference between two water pressures P_w and P_w^{sat}. At high cell current densities, water moves from anode side to the cathode side and as shown in Fig. 6, the water mole fraction will increase at the GDL/CL interface. High water mole fraction results in high P_w. Therefore, the region with the high condensation is close to the GDL/CL interface.
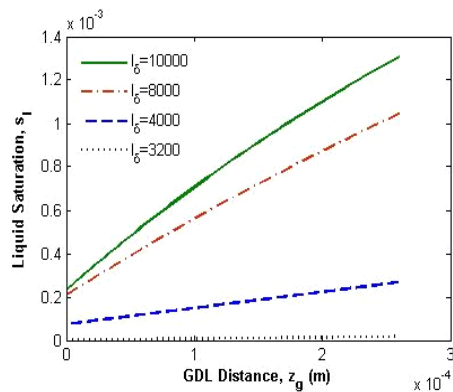

Figure 9: Variation of liquid water saturation with current density for different I_δ (A/m^2).

Fig. 9 also shows that at the minimum value of $I_\delta =$ 3200 A/m^2, condensation occurs throughout the GDL. This value is reported as $I_\delta =$ 3900 A/m^2 by You and Liu [4] that considered two phase flow through the GDL and a separate equation for liquid water in terms of capillary pressure.

7. CONCLUSION

An algorithm for water management in the cathode side of the PEMFC wad developed. The net water transported coefficient through the membrane decreases from the cathode side to anode side because of the decreasing of electro-osmotic drag coefficient. The net water transported coefficient depends on the cell current density, water activity and water partial pressure. Electro-osmotic drag has the main contribution to the net water flux transported through the membrane. The results approved that for the base case conditions, no liquid water exists until 3200 A/m^2. The amount of water condensation becomes much more at the GDL/CL interface than other regions of GDL.

8. NOMENCLATURE

A	Area
C	Concentration
D	Diffusivity
F	Faraday constant, 96485 coulombs/mol
I_δ	Cell current density
J	Diffusive flux
K	Hydraulic permeability
l_g	GDL thickness
l_m	Membrane thickness
M	Molecular weight
N	Molar flux
P	Pressure
$\bar{R}$	Universal gas constant, 8.314 J/ (mol K)
T	Temperature
a	Water activity
x	Mole fraction

Greek Letters

α	Net water transport coefficient
δ	Kronecker delta
ε	Porosity
λ	Membrane water content
μ	Dynamic viscosity
ξ	Stoichiometric coefficient
ρ	Density
υ	Gas mixture velocity
ϕ	Relative humidity
κ	Protonic conductivity
σ	Electronic conductivity

Super scripts

l	Liquid phase
sat	Saturation state

Sub scripts

c	Cathode side
$diff$	Diffusion
$drag$	Electro-osmotic drag
F	Fickinan value
g	GDL
hyd	Hydraulic
in	Inlet
m	Membrane
W	Water

10. REFERENCES

[1] D. M. Bernardi and M. W. Verbrugge, "Mathematical Model of a Gas Diffusion Electrode Bonded to a Polymer Electrolyte," *AIChE J., 37(9),* pp. 1151–1163, 1991.

[2] T. E. Fuller and J. Newman, "Water and Thermal Management in Solid-Polymer-Electrolyte Fuel Cells," *J. Electrochem. Soc., 140,* pp. 1218–1225, 1993.

[3] T. E. Springer, T. A. Zawodzinski, and S. Gottefeld, "Polymer Electrolyte Fuel Cell Model," *J. Electrochem. Soc., 138 (8),* pp. 2334–2342, 1991.

[4] L. You and H. Liu, "A Two-Phase and Transport Model for the Cathode of PEM Fuel Cells," *Int. J. Heat and Mass Transfer, 45* pp. 2277–2287, 2002.

[5] M. J. Kermani and J. M. Stockie, "Heat and Mass Transfer Modeling of Dry Gases in the Cathode of PEM Fuel Cells," *Int. J. Comp. fluid dyn., 18(2),* pp. 153–164, 2004.

[6] R. E. De la Rue and C. W. Tobias, "On the Conductivity of Dispersions," *J. Electrochem. Soc., 106,* pp. 827–833, 1959.

[7] E. L. Cussler, Diffusion Mass Transfer in Fluid Systems, Cambridge University Press, 1984.

[8] Ugur Pasaogullari, C.Y. Wang and Ken S. Chen. "Two-Phase Transport in Polymer Electrolyte Fuel Cells with Bilayer Cathode Gas Diffusion Media," *J. Electrochem. Soc., 152(8),* pp. 1574–1582, 2005.

[9] S. Motupally, A. J. Becker and J. W. Weidner, "Diffusion of Water in Nafion 115 Membranes," *J. Electrochem. Soc., 147(9)*, pp. 3171–3177, 2000.

[10] Weber, A.Z. and Newman, J., "Modeling Transport in Polymer-Electrolyte Fuel Cells", *Chem. Rev*., *104*, pp. 4679–4726, 2004.

[11] J. Larminie, and A. Dicks, Fuel Cell Systems Explained, John Wiley and Sons, 2001.

[12] Ticianelli E.A., Derouin C.R., Redondo A., Srinivasan S., "Methods to Advance Technology of Proton Exchange Membrane Fuel Cells" J. *Electrochem. Soc. 135* pp*. (1988) 2209*.